

Sketch-in-Latents: Eliciting Unified Reasoning in MLLMs

Jintao Tong¹ Jiaqi Gu² Yujing Lou² Lubin Fan^{2†} Yixiong Zou^{1†}
Yue Wu² Jieping Ye² Ruixuan Li^{1†}

¹School of Computer Science and Technology, Huazhong University of Science and Technology
²Alibaba Cloud Computing [†]Corresponding authors

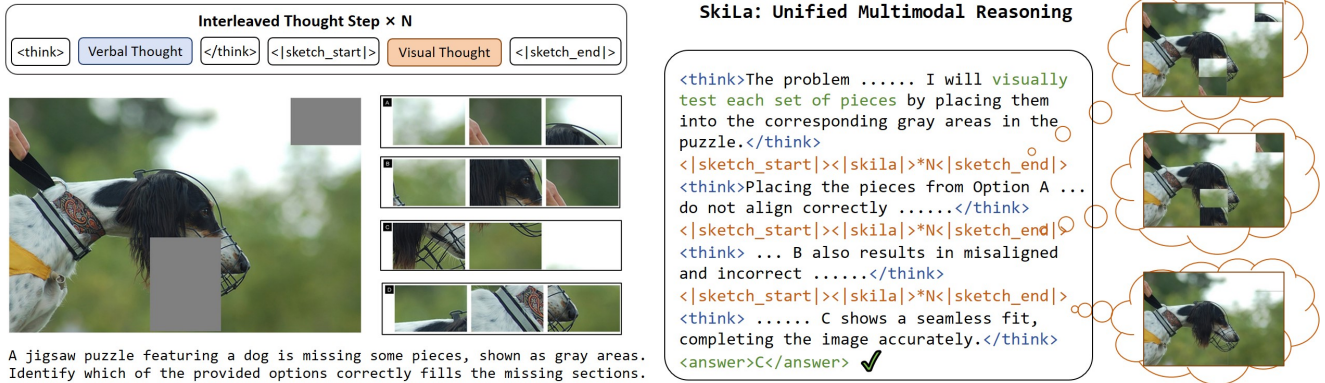


Figure 1. SkiLa empowers MLLMs to think in a unified manner through a hybrid auto-regressive process, generating multi-step, interleaved multi-modal reasoning traces, enabling the model to flexibly think with unpredefined visual-text imagination and interactions. It dynamically alternates between the textual thinking mode to generate textual thoughts and the visual sketching mode to generate latent sketch tokens as visual thoughts, effectively solving challenging tasks that current linguistic-CoT-based methods fail.

Abstract

While Multimodal Large Language Models (MLLMs) excel at visual understanding tasks through text reasoning, they often fall short in scenarios requiring visual imagination. Unlike current works that take predefined external toolkits or generate images during thinking, however, humans can form flexible visual-text imagination and interactions during thinking without predefined toolkits, where one important reason is that humans construct the visual-text thinking process in a unified space inside the brain. Inspired by this capability, given that current MLLMs already encode visual and text information in the same feature space, we hold that visual tokens can be seamlessly inserted into the reasoning process carried by text tokens, where ideally, all visual imagination processes can be encoded by the latent features. To achieve this goal, we propose Sketch-in-Latents (SkiLa), a novel paradigm for unified multi-modal reasoning that expands the auto-regressive capabilities of MLLMs to natively generate continuous visual embeddings, termed latent sketch tokens, as visual thoughts. During multi-step reasoning, the model dynamically alternates between textual thinking mode for generating textual think to-

kens and visual sketching mode for generating latent sketch tokens. A latent visual semantics reconstruction mechanism is proposed to ensure these latent sketch tokens are semantically grounded. Extensive experiments demonstrate that SkiLa achieves superior performance on vision-centric tasks while exhibiting strong generalization to diverse general multi-modal benchmarks. Codes will be released at <https://github.com/TungChintao/SkiLa>.

1. Introduction

In recent years, multi-modal large language models (MLLMs) [3, 21, 24, 40] have made remarkable progress by coupling powerful visual encoders with the generative capabilities of large language models (LLMs) [2, 7, 35]. Building on the success of Chain-of-Thought (CoT) reasoning in LLMs [41], recent multi-modal research [16, 28, 51] has adopted this step-by-step reasoning to effectively decompose and solve complex visual-referenced queries.

However, a fundamental limitation persists: the reasoning process of these multi-modal reasoning models is majorly restricted to the linguistic domain [38, 48]. Even when processing images, their inference unfolds solely as a se-

quential generation of text tokens. This text-centric bottleneck forces them to verbalize problems that humans would solve intuitively through mental visualization. This limitation stands in sharp contrast to human cognition, where linguistic reasoning is naturally and seamlessly interleaved with internal visual imagination [10, 17]. For tasks demanding rich visual-spatial intuition (e.g. jigsaw, object localization) [12], this limitation becomes particularly pronounced.

Recent efforts to address this gap have explored two main directions. The first introduces tool-driven visual exploration [27, 29, 42, 50, 54] and programmatic visual manipulation [15, 53]. Tool-based methods enable models to call external utilities for visual interaction, while programmatic approaches generate executable code to perform operations on images, such as drawing auxiliary lines or applying transformations. Although an important step, this approach still relies on predefined toolkits or code execution criterion with limited action spaces, unlike humans to flexibly conduct unlimited visual-text imagination or counterfactual visual-text reasoning. The second direction explores unified foundation models [5, 8, 32] that generate outputs in both text and images. However, they incur substantial computational costs due to detailed image generation pipelines, which is often constrained by their generative capability. Moreover, their effectiveness has been validated so far only in specific downstream tasks [20, 45] such as navigation and maze solving, limiting their generalizability.

Unlike current works, one important reason for humans’ unlimited visual-text imagination capability is that the visual-text interaction occurs in an internal and unified space inside the human brain. A fundamental question then emerges: *Can MLLMs transcend their linguistic reasoning framework to generate visual thoughts natively as part of an internal, unified reasoning process?* This question motivates our goal: enabling MLLMs to internally generate continuous embeddings that natively represent visual thoughts. Since in MLLMs, images and texts are all encoded by the LLM into the same feature space, intuitively, to achieve our goal, we hold that **visual tokens should be able to be seamlessly inserted into the reasoning process carried by text tokens**, forming the internal and unified reasoning process. Two straightforward advantages of this motivation are: (1) all kinds of visual imaginations can be represented by token features, leading to unlimited visual-thinking manners; (2) the model can seamlessly forming an interleave visual-text reasoning trace, which leads to a more flexible and human-like thinking process.

Based on these insights, drawing inspiration from CoCoT [13] in the text domain that leverages the LLM’s last hidden states as latent text thoughts, we propose Sketch-in-Latents (SkiLa), a novel paradigm for unified multi-modal reasoning that expands the auto-regressive capabilities of MLLMs to natively generate continuous visual embed-

dings, termed latent sketch tokens, to act as visual thoughts. Specifically, SkiLa empowers MLLMs to think in a unified manner through a hybrid auto-regressive process, generating multi-step, interleaved multi-modal reasoning traces. It dynamically alternates between: (1) *Textual thinking mode*: standard next-token prediction on discrete text tokens for textual thoughts, and (2) *Visual sketching mode*: continuous latent sketch token generation for visual thoughts. To ensure these latent sketch tokens are semantically grounded, we introduce a latent visual semantics reconstruction mechanism. We leverage interleaved text-image reasoning data containing intermediate “sketch images” that represent steps in a visual thought process. A sketch encoder extracts visual embeddings from these sketches to serve as reconstruction targets. The MLLM is then trained to generate this interleaved sequence: performing standard next-token prediction for textual thoughts and generating latent visual tokens that reconstruct the visual semantics for sketch thoughts.

Extensive experiments validate that SkiLa equips the model with an intrinsic unified reasoning capability. As in Figure 1, SkiLa can initiate its reasoning linguistically, seamlessly transition to visual sketching mode to perform visual simulations and manipulate visual concepts directly within its latent space, and then revert to text generation. This establishes a novel and flexible paradigm for multi-step unified reasoning where visual cognition and linguistic thoughts are deeply integrated.

Our contributions are summarized as follows:

- We propose Sketch-in-Latents (SkiLa), a novel unified reasoning paradigm that enables a hybrid auto-regressive process, allowing MLLMs to flexibly and seamlessly interleave multi-step explicit textual thoughts and latent visual thoughts without pre-defined external actions.
- We introduce a general-purpose latent visual semantics reconstruction mechanism that trains models to generate meaningful visual representations by reconstructing visual semantics from intermediate sketch images, effectively creating intermediate intrinsic visual thoughts.
- We demonstrate our method’s effectiveness and generality, showing it not only achieves state-of-the-art results on vision-centric tasks but also exhibits strong generalization and improves performance on diverse general multi-modal benchmarks.

2. Related Works

2.1. Multi-modal Chain-of-Thought

Chain-of-Thought (CoT) [41] improves LLM’s reasoning by decomposing complex problems into intermediate steps. Recent works [14, 22, 38, 46, 48] have extended this paradigm to multi-modal settings, with methods like Vision-R1 [16] and Visual-RFT [28] training MLLMs for step-by-step reasoning. However, their reasoning are forced

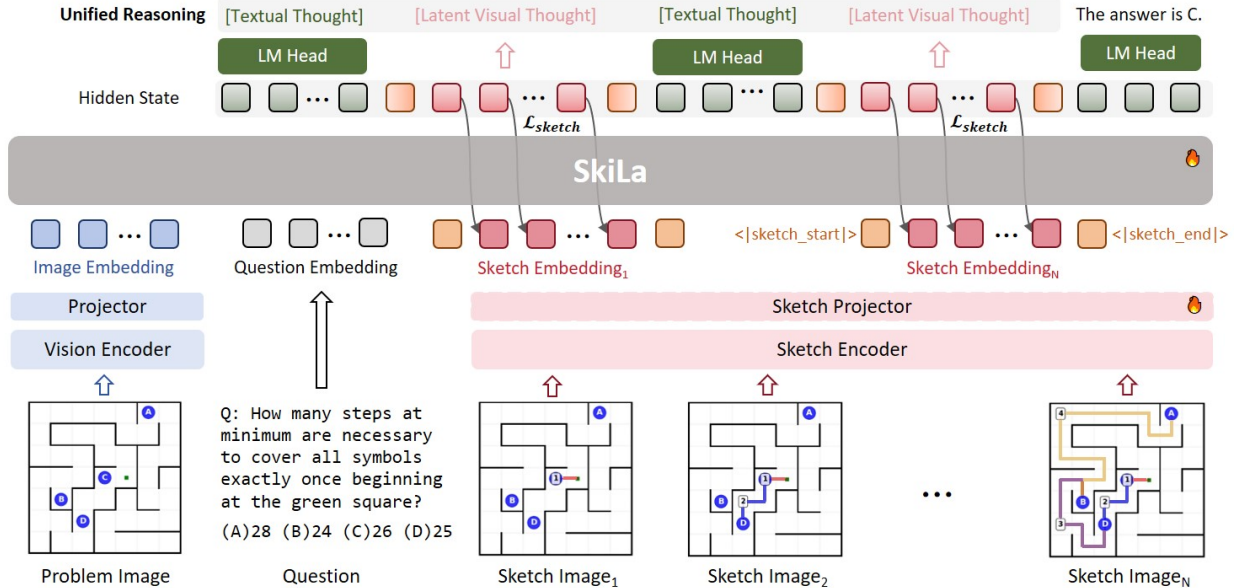


Figure 2. The training and inference of SkiLa. It dynamically alternates between textual thinking mode to generate textual thoughts and visual sketching mode to generate latent sketch tokens as visual thoughts. During training, the latent visual semantics reconstruction mechanism leverages a sketch module (encoder and projector), used exclusively during training, to extract visual embeddings from sketch images as reconstruction targets, ensuring the latent sketch tokens are semantically grounded.

to verbalize visual concepts in the linguistic domain, which hinders their performance on vision-intensive tasks.

Existing efforts to enable “think with images” fall into two categories. Tool-driven methods [29, 42, 53] equip MLLMs with predefined external utilities for actions like cropping, drawing, or marking regions. Visual Sketchpad [15], for instance, generates code to produce auxiliary visual aids, while DeepEyes [54] generates bounding boxes and then employs zoom-in tools to crop images for better reasoning. While effective to an extent, these methods depend on predefined tool-kits with fixed action spaces, limiting flexibility, and failing to cultivate an intrinsic reasoning faculty. A second direction pursues unified foundation models like Janus-Pro [5] and Bagel [8], which interleave text and image generation within reasoning chains. However, this paradigm is hampered by the prohibitive cost of pixel-level synthesis. Moreover, their understanding is bounded by their generative fidelity, meaning they cannot reason about what they cannot draw. Their effectiveness has also been shown mainly in specific domains such as navigation and maze solving [20, 45], raising concerns about their generalizability. In contrast, SkiLa natively generates intrinsic visual thoughts, eliminating dependencies on external tools or costly pixel-level generation pipelines.

2.2. Latent Reasoning

Several studies have explored performing reasoning in a continuous embedding space rather than discrete token space [6, 13, 30, 52] to improve the reasoning efficiency of

LLMs. Recent work extends latent reasoning to MLLMs. For instance, Mirage [47] employs hidden states trained to approximate annotated auxiliary visual information, while LVR [19] learns to reason over reconstructed image crops within the latent space. However, these methods suffer from two limitations. First, they focus exclusively on visual-only reasoning, failing to interleave it with textual thoughts. This separation significantly reduces interpretability because the reasoning process is opaque, providing neither intermediate images for inspection nor corresponding textual explanations. Second, their reasoning is typically confined to a single inferential step, which limits their applicability to complex, multi-step downstream tasks. In contrast, our paradigm enables a multi-step, interleaved reasoning trace through a hybrid auto-regressive process, dynamically alternating between textual and visual thoughts.

3. Methods

In this section, we introduce Sketch-in-Latents (SkiLa), a novel reasoning paradigm that enables MLLMs to reason jointly over discrete text and continuous visual representations within a unified auto-regressive process. The overall training pipeline is illustrated in Figure 2. Unlike methods that require predefined external tools or image generation pipelines, SkiLa seamlessly alternates between two distinct operational modes: a textual thinking mode, which generates textual thoughts via standard next-token prediction, and a visual sketching mode, which produces sequences of continuous latent sketch tokens as visual thoughts.

3.1. SkiLa: Sketch-in-Latents

3.1.1. Model Architecture

The SkiLa architecture is built upon a standard MLLM framework, comprising three components: a vision encoder E_v mapping input images \mathbf{I} to visual tokens $\mathbf{V} = E_v(\mathbf{I})$; a modality projector $proj$ aligning \mathbf{V} to the LLM’s embedding space ($\mathbf{V}_e = proj(\mathbf{V})$); and an LLM backbone θ that auto-regressively generates responses conditioned on \mathbf{V}_e and textual embeddings \mathbf{T} .

To enable latent sketching, SkiLa introduces a sketch module, which is used exclusively during training. This module, consisting of a sketch encoder E_s and projector $proj_s$, encodes intermediate “sketch images”(i.e., visual thoughts) \mathbf{I}_s from the training data to generate the visual semantic reconstruction targets $\mathbf{V}_s = proj_s(E_s(\mathbf{I}_s))$.

3.1.2. Hybrid Auto-Regressive Process

The SkiLa’s LLM backbone is trained to perform a hybrid auto-regressive process to achieve unified internal reasoning. The model generates special tokens, $\langle |sketch_start| \rangle$ and $\langle |sketch_end| \rangle$, to switch reasoning modes. Upon generating $\langle |sketch_start| \rangle$, the model enters “visual sketching mode”, where it auto-regressively generates a sequence of continuous latent sketch visual tokens $\mathbf{H}_{sketch} = \{\mathbf{h}_1, \dots, \mathbf{h}_K\}$, trained to reconstruct the visual thought semantics \mathbf{V}_s . Upon generating $\langle |sketch_end| \rangle$ seamlessly resumes standard next-token prediction for generating textual thoughts.

Specifically, given an image-question pair (\mathbf{I}, \mathbf{Q}) , SkiLa performs reasoning by a hybrid auto-regressive process and gets the final answer. It can generate a unified reasoning trace $\mathcal{S} = \{s_1, \dots, s_N\}$, where

$$s_i \sim \mathcal{P}_\theta(s|\mathbf{V}_e, \mathbf{T}, s_1, \dots, s_{i-1}), \quad s_i \in \{t_i, h_i\}.$$

s_i can be either text token t_i or latent sketch token h_i . Special tokens are omitted from the notation for simplicity.

3.2. Unified Training Objective

Our training objective is to jointly optimize the model’s ability to generate coherent text and meaningful latent visual semantics, supervised over an interleaved reasoning trace containing textual thoughts \mathbf{X}_t and sketch images \mathbf{I}_s (i.e., visual thoughts).

For each textual thought \mathbf{X}_t , the target is the standard sequence of text tokens \mathbf{T}_t . For each sketch image \mathbf{I}_s , we formulate a concise visual target. First, the sketch encoder E_s extracts patch-level features, resulting in M tokens (e.g., 729 tokens for SigLIP2). These features are then projected into the LLM’s embedding space by the sketch projector $proj_s$. To balance the length of visual thoughts with textual thoughts and to provide concise visual semantics for supervision, we apply average pooling to compress the projected

features into a fixed-size sequence of K salient vectors (e.g., $K = 27$). The final visual reconstruction target sequence is thus $\mathbf{V}_s = \{\mathbf{v}_{s,1}, \dots, \mathbf{v}_{s,K}\}$. We then train the LLM backbone θ with a two-part objective:

Latent Sketch Reconstruction Loss When the model is in latent sketching mode (i.e., $\langle |sketch_start| \rangle$ is generated), it is trained to auto-regressively generate a sequence of K latent sketch tokens, $\mathbf{H}_{sketch} = \{\mathbf{h}_1, \dots, \mathbf{h}_K\}$. This is achieved by propagating the last hidden state from the previous step as the input embedding for the current step. We enforce these generated latent sketch tokens to approximate the ground-truth visual semantics \mathbf{V}_s using a mean squared error (MSE) objective:

$$\mathcal{L}_{Sketch} = \frac{1}{K} \sum_{j=1}^K \|\mathbf{h}_j - \mathbf{v}_{s,j}\|_2^2$$

where \mathbf{h}_j is the j -th generated latent sketch token and $\mathbf{v}_{s,j}$ is the j -th target vector from \mathbf{V}_s . The parameters of the sketch projector $proj_s$ are jointly trained via this reconstruction loss, without needing a separate training process.

Next-Token Prediction (NTP) Loss For all discrete tokens (including special tokens, textual thoughts \mathbf{X}_t , and the final answer \mathbf{X}_A), we apply a standard cross-entropy loss. A sketch mask is apply to ensure this loss will be not applied to the latent sketch tokens that enclosed in special tokens $\langle |sketch_start| \rangle$ and $\langle |sketch_end| \rangle$.

$$\mathcal{L}_{NTP} = - \sum_{t_i} \log p_\theta(t_i|\mathbf{V}_e, \mathbf{T}, s_{1:i}).$$

Joint Objective The final training loss for SkiLa is a weighted sum of these two components, balanced by a hyperparameter λ_{Sketch} :

$$\mathcal{L}_{SkiLa} = \mathcal{L}_{NTP} + \lambda_{Sketch} \cdot \mathcal{L}_{Sketch}$$

3.3. Inference with Unified Reasoning

For inference, the entire sketch module (E_s and $proj_s$) is discarded, incurring zero additional parameter or computational cost compared to a standard MLLM.

Inference proceeds in a hybrid auto-regressive manner as an unified process. The model begins by generating text tokens in response to the input image \mathbf{I} and question \mathbf{Q} , sampling from its standard vocabulary. Upon sampling $\langle |sketch_start| \rangle$, the decoding logic switches to “latent sketching mode”. In this mode, the model propagates its last hidden state as the input embedding for the next step, auto-regressively generating a sequence of latent sketch tokens \mathbf{H}_{sketch} . This latent generation continues until $\langle |sketch_end| \rangle$ is sampled.

During inference, the model may generate more latent sketch tokens than the fixed training length K . Therefore,

we impose a maximum limit: if the generated sketch tokens exceed twice the training length (i.e., $2K$), the model is forced to exit the latent sketch mode. This prevents excessively long visual thoughts from overshadowing textual reasoning. Upon exiting the latent sketch mode (by sampling `<|sketch_end|>` or reaching the limit), the model seamlessly resumes standard next-token prediction. The internally generated latent sketch tokens \mathbf{H}_{sketch} function as the model’s visual thought, conditioning subsequent language generation without ever being decoded into pixels.

4. Experiments

Training Details We adopt Qwen2.5-VL 7B [3] as the base model. The sketch module, which is used only for training-time supervision and discarded at inference, employs a SigLIP2-So/14-384 [36] as the default sketch encoder and a single-layer MLP as the sketch projector. The parameters of the base vision encoder, sketch encoder and multi-modal projector are kept frozen, with only the LLM and sketch projector parameters updated. We perform supervised fine-tuning for 1 epoch on $8 \times A100-80G$ GPUs with a batch size of 128. A cosine learning rate scheduler is applied with an initial learning rate of $1e-5$ for LLM and $1e-4$ for sketch projector. In addition to **SkiLa**, trained on interleaved textual and visual thoughts with unified reasoning, we report **SkiLa-V**, a purely visual reasoning version trained on the same dataset without textual thoughts.

Training Data Our SFT training data is curated from the Zebra-CoT [18], which is a diverse large-scale dataset with 182K samples, containing logically coherent interleaved text-image reasoning traces. We filter this dataset to select samples suitable for SkiLa training, excluding 3D data and instances where the intermediate sketch images are too complex for the MLLM to effectively learn to reconstruct. Consequently, our training dataset contains 101K samples. The selected data is then reformatted into an interleaved sequence of textual thoughts and visual sketch targets, following the structure shown in Figure 3:

```

SkiLa Training Sample
Interleaved Textual and Visual Thoughts
<think> [Textual Thought 1] </think>
<|sketch_start|> [Sketch Image 1] <|sketch_end|>
<think> [Textual Thought 2] </think>
<|sketch_start|> [Sketch Image 2] <|sketch_end|>
... ..
<think> [Textual Thought N] </think>
<|sketch_start|> [Sketch Image N] <|sketch_end|>
<think> [Final Textual Thought] </think>
<answer> [Final Answer] </answer>

```

Figure 3. The format structure of the SkiLa training sample.

4.1. Evaluation Benchmarks and Baselines

Evaluation Benchmarks We evaluate SkiLa on a comprehensive suite of vision-centric and multimodal benchmarks to assess its visual perception and reasoning capabilities under diverse settings. For vision-centric evaluation, we adopt MMVP [34], RealWorldQA (RWQA) [44], BLINK [12], V*Bench (V*) [43], HRBench (HR_{4K} and HR_{8K}) [39], and MME-RealWorld-Lite [49]. These benchmarks focus on fine-grained visual perception, visual reasoning, and high-resolution image understanding, covering challenging scenarios such as visual illusions, real-world complexity, and detailed spatial reasoning. For multimodal evaluation, we further test SkiLa on MMStar [4] and MMBench [26], which evaluate general-purpose multimodal reasoning in multi-choice settings.

Baselines To comprehensively evaluate our approach, we benchmark SkiLa against a carefully selected suite of baselines. First, to isolate the impact of our proposed reasoning framework from the training data itself, we establish a Direct SFT baseline, which is a text-only SFT variant trained on the exact same dataset and with identical parameters as SkiLa. We then introduce several state-of-the-art models. For comparison against alternative visual supervision techniques, we include ROSS [37], which employs a denoising objective to reconstruct the input image, and Janus-Pro [5], a unified model capable of in-line image generation. For reasoning-centric comparisons, we include Vision-R1 [16], which improves textual CoT with reinforcement learning, and LVR [19], which performs latent-space reasoning by reconstructing the semantics of regions of interest. In Table 1, * denotes the results reproduced by ourselves, while all other results [1, 25, 33] are obtained from the OpenVLM [9] and BLINK [12] leaderboards.

4.2. Main Results

4.2.1. Vision-Centric and Multimodal Tasks

The comprehensive evaluation results on vision-centric and multimodal multi-choice tasks are presented in Table 1. Overall, our models consistently outperform the Qwen2.5-VL 7B baseline across all evaluated benchmarks, covering vision-centric perception, high-resolution understanding, and multimodal reasoning tasks. The results highlight some key findings that validate our approach: **(1) Visual semantics reconstruction boosts overall performance on visually intensive tasks.** A key observation is that for tasks demanding fine-grained visual discernment, our SkiLa-V provides substantially larger gains than other reasoning methods. This suggests that linguistic descriptions are often insufficient to capture the full spectrum of visual information. In contrast, visual semantics reconstruction enables the model to effectively imagine such visual details. For instance, in the BLINK subtask “Jigsaw Puz-

Methods	MMVP	MMStar	MMBench	RWQA	BLINK	V*	HR _{4K}	HR _{8K}	MME-RealWorld-Lite		
									Perception	Reasoning	Overall
<i>Close Source Models</i>											
GPT-4o	70.7	61.6	82.1	68.6	60.0	66.0	59.0	55.5	54.4	48.3	52.0
GPT-4v	-	56.0	81.0	63.0	58.3	-	-	-	-	-	-
GPT-4o-mini	-	54.8	77.6	67.1	53.6	-	-	-	38.8	35.2	37.4
Claude3.7-Sonnet	-	65.1	81.4	55.4	56.6	-	-	-	-	-	-
<i>Open Source Models</i>											
Gemma3 27B	-	59.6	82.3	62.5	53.5	-	-	-	-	-	-
Cambrian 13B	41.3	47.1	73.4	58.6	43.1	-	-	-	-	-	-
Janus-Pro 7B	63.3	46.5	62.6	42.7	38.7	-	-	-	-	-	-
LLaVA-OneVision 7B	-	61.9	83.2	-	53.0	75.4	63.0	59.8	52.8	42.7	48.5
Qwen2.5-VL 7B	66.0	60.3	82.5	67.4	55.1	78.5	68.5	65.0	48.6	37.7	44.3
Direct SFT	70.2	61.4	82.1	68.1	56.1	69.1	65.9	61.0	49.6	44.3	47.5
ROSS 7B [37]	49.3	53.9	80.5	58.7	45.3	-	-	-	-	-	-
Vision-R1 7B* [16]	72.6	60.7	79.8	67.1	51.0	80.1	64.8	57.0	49.8	44.9	47.9
LVR 7B* [19]	72.0	61.3	74.6	67.7	52.5	81.7	69.6	66.1	52.7	43.5	49.1
SkiLa-V	72.0	64.5	82.4	70.5	56.7	79.6	68.5	65.2	51.7	47.7	50.2
Δ (vs Qwen2.5-VL 7B)	+6.0	+4.2	-0.1	+3.1	+1.6	+1.1	+0.0	+0.2	+3.1	+10.0	+5.9
SkiLa	75.3	64.8	83.3	69.3	56.7	84.3	72.0	66.5	56.6	50.2	54.1
Δ (vs Qwen2.5-VL 7B)	+9.3	+4.5	+0.8	+1.9	+1.6	+5.8	+3.5	+1.5	+8.0	+12.5	+9.8

Table 1. **Experimental results on various vision-centric and multimodal multi-choices tasks.** Our SkiLa with “Unified Reasoning” paradigm outperforms both “Textual Reasoning” and “Visual Reasoning” paradigms. Here, * denotes the results test by ourselves.

Methods	TextVQA	MME			POPE			
		Perception	Cognition	Overall	Adversarial	Popular	Random	Overall
Qwen2.5-VL 7B	77.5	1691.4	623.5	2314.9	85.5	86.5	87.2	86.4
Direct SFT	76.1	1536.5	646.8	2183.3	82.4	83.2	84.4	83.3
LVR 7B [19]	75.6	1496.1	539.6	2035.7	83.4	84.2	85.1	84.2
SkiLa-V	80.8	1636.9	646.5	2283.4	85.8	86.7	87.8	86.8
Δ (vs Qwen2.5-VL 7B)	+3.3	-3.2%	+3.7%	-1.3%	-0.1	+0.2	+0.6	+0.3
SkiLa	79.3	1708.9	695.4	2404.3	86.4	87.4	88.2	87.3
Δ (vs Qwen2.5-VL 7B)	+1.8	+1.0%	+11.5%	+3.9%	+0.9	+0.9	+1.0	+0.9

Table 2. Results on VQA and Hallucination Benchmarks. SkiLa demonstrates strong generalization across diverse multi-modal tasks.

zle”, shown in Figure 1, success hinges on the holistic coherence of the assembled image, which is more natively and effectively represented through visual simulation. **(2) Unified reasoning sets the best performance by leveraging modality complementarity.** As evidenced by our results, SkiLa consistently achieves best performance, outperforming all single-modality reasoning approaches in our comparison. Notably, it also surpasses leading proprietary models such as GPT-4o and Claude3.7-Sonnet. We attribute this success to our unified paradigm’s ability to harness the complementary strengths of both modalities: it effectively fuses the imaginative, holistic nature of visual thought with the structured, sequential deliberation of textual thought. This outcome highlights the superior scalability and effectiveness of a truly unified reasoning process for MLLMs.

4.2.2. General Tasks

Our SkiLa not only achieves state-of-the-art performance on vision-centric benchmarks, but also demonstrates strong generalization across diverse multi-modal tasks. To further assess its generalization, we evaluate SkiLa on several out-of-domain benchmarks, including TextVQA [31], MME [11], and POPE [23]. TextVQA focuses on the integration of textual information within images, testing the model’s ability to align visual and linguistic cues. MME provides a comprehensive assessment of perceptual and cognitive abilities across multi-modal understanding. The POPE benchmark systematically evaluates object hallucination in MLLMs.

As shown in Table 2, while the Direct SFT baseline, trained on the same dataset but without reasoning trajec-

Methods	Sketch Token Num	MMVP	MMStar	MMBench	RWQA	BLINK	V*	MME-RealWorld-Lite		
								Perception	Reasoning	Overall
Qwen2.5-VL 7B	-	66.0	60.3	82.5	67.4	55.1	78.5	48.6	37.7	44.3
<i>Visual Reasoning (SkiLa-V)</i>										
SkiLa-QwenViT	28	68.3	64.4	81.9	69.3	56.2	79.2	49.8	44.9	47.9
SkiLa-CLIP	24	72.0	64.5	82.5	70.6	56.0	79.3	50.7	46.1	48.9
SkiLa-SigLIP2	27	72.0	64.5	82.4	70.5	56.7	79.6	51.7	47.7	50.2
<i>Unified Reasoning (SkiLa)</i>										
SkiLa-QwenViT	28	73.3	62.3	82.8	68.1	55.8	81.5	52.7	47.3	50.6
SkiLa-CLIP	24	73.0	63.4	83.0	68.5	55.5	82.1	52.5	46.7	50.2
SkiLa-SigLIP2	27	75.3	64.8	83.3	69.3	56.7	84.3	56.6	50.2	54.1

Table 3. Impact of different sketch encoders for generating latent visual semantics as the SFT reconstruction target.

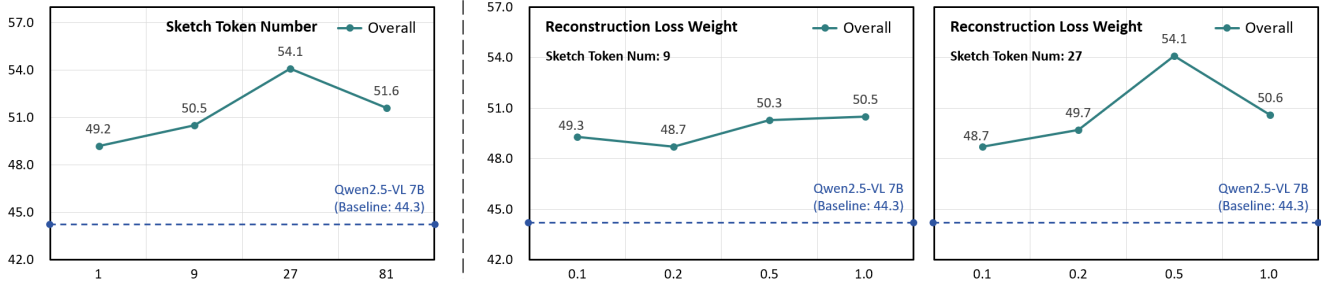


Figure 4. Test on MME-RealWorld-Lite. (Left) Impact of reconstructed sketch visual token count on model performance. (Middle and Right) Impact of the latent sketch reconstruction loss weight with 9 and 27 sketch tokens on model performance.

tories, exhibits noticeable performance drops, our method delivers substantial gains. In particular, SkiLa-V and SkiLa demonstrate strong text-grounded reasoning, outperforming the baseline by +3.3 and +1.8 on TextVQA. More importantly, SkiLa consistently achieves the best overall performance, enhancing perceptual and cognitive reasoning (+3.9% on MME) and improving factuality by reducing hallucinations (+0.9 on POPE). These results collectively confirm that SkiLa not only excels in its primary reasoning objectives but also generalizes effectively, enhancing both multi-modal understanding and factual alignment.

4.3. Ablation Studies

Choice of Sketch Encoder We investigate the impact of different sketch encoders for generating the visual reconstruction target in Table 3. The core question is whether the architectural consistency of the native QwenViT is more beneficial than the richer semantic features from powerful, contrastively pre-trained external encoders like CLIP and SigLIP2. To ensure a fair comparison, we select a comparable number of sketch tokens for each: 28 for QwenViT, 24 for CLIP, and 27 for SigLIP2. The results decisively favor external encoders, with SigLIP2 achieving the highest scores in almost benchmarks on SkiLa-V and SkiLa. This demonstrates that the superior feature generality from a powerful, independently trained model is more critical than

architectural consistency. Based on its top performance, we adopt SigLIP2 as our default.

Choice of Sketch Encoder We investigate the impact of different sketch encoders for generating the visual reconstruction target in Table 3. The core question is whether architectural consistency with the native QwenViT is more beneficial than the richer semantic features provided by powerful, contrastively pre-trained external encoders such as CLIP and SigLIP2. To ensure a fair comparison, we select a comparable number of sketch tokens for each encoder: 28 for QwenViT, 24 for CLIP, and 27 for SigLIP2. The results decisively favor external encoders, with SigLIP2 achieving the highest scores on almost all benchmarks for both SkiLa-V and SkiLa. This demonstrates that superior feature generality from a powerful, independently trained model is more critical than architectural consistency. Based on its top performance, we adopt SigLIP2 as our default.

Impact of sketch token number We study how the number of reconstructed sketch visual tokens affects model performance. As illustrated in Figure 4 (left), our method consistently outperforms the baseline across a wide range of token counts, from 1 to 81. Performance improves steadily as the number of visual tokens increases, reaching its peak at 27 tokens. Beyond this point, a slight performance drop is observed at 81 tokens. Empirically, 27 tokens yield the best average performance, suggesting that increasing the number

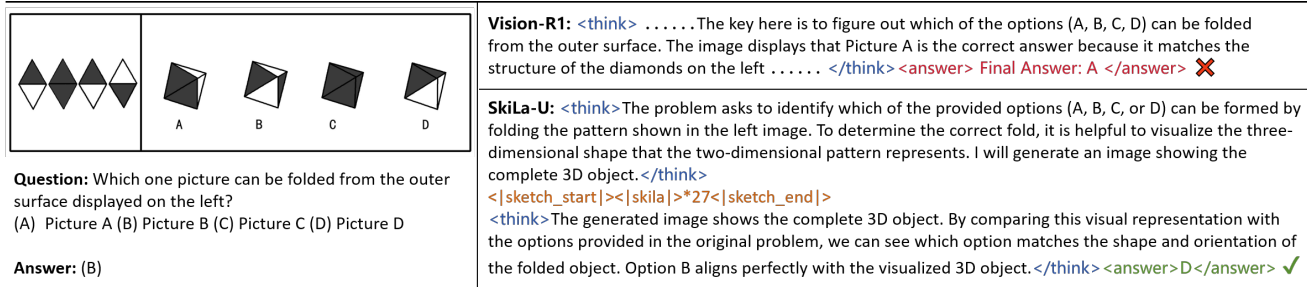


Figure 5. An example of spatial imagination. SkiLa generates visual thoughts to imagine the 3D object from a 2D pattern.

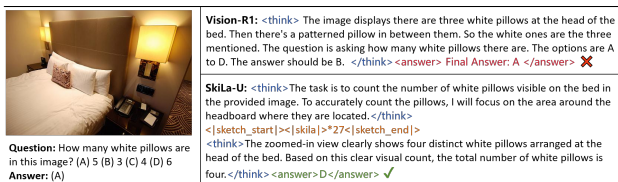


Figure 6. An example of hallucination mitigation.

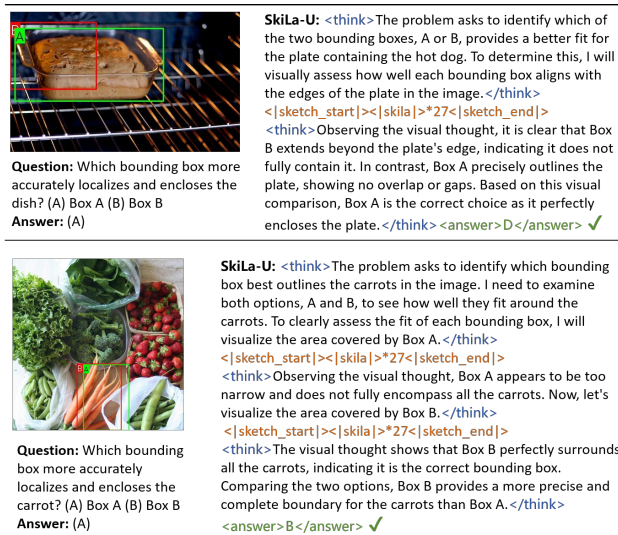


Figure 7. An example of adaptive unified reasoning.

of sketch visual tokens does not always lead to further gains. Introducing too many visual tokens may reduce the relative contribution of textual reasoning, highlighting the need to balance visual and textual thoughts. Therefore, to maintain a proper balance between visual and textual thoughts, we choose 27 sketch visual tokens as the default number.

Latent Sketch Reconstruction Loss Weight We evaluate the effect of reconstruction loss weights (0.1–1.0) on the model’s average performance across vision-centric tasks, considering two configurations of sketch token numbers, 9 and 27, to analyze their interaction with the loss weight. As shown in Figure 4 (middle), with fewer sketch tokens (9), the model is robust to variations in loss weight, exhibiting

only a marginal performance change. With more sketch tokens (27), stronger supervision becomes essential (Figure 4, right), as insufficient loss weight limits the generation of meaningful sketch tokens and leads to suboptimal performance. These results indicate that the optimal loss weight should align with the number of sketch tokens to ensure effective latent sketch supervision. Based on this, we set 0.5 as the default latent sketch reconstruction loss weight.

4.4. Discussion

Beyond quantitative metrics, our evaluation revealed several remarkable emerging capabilities. We now explore these phenomena through detailed case analyses.

Spatial Imagination Pure text-based reasoning methods consistently fail on spatial tasks, primarily due to the inherent ambiguity of representing complex 3D geometric properties textually. In contrast, SkiLa overcomes this limitation by generating visual thoughts to mentally simulate the 3D object represented by a 2D pattern, and then uses this mental visualization to compare with candidate options and identify the correct fold, as illustrated in Figure 5.

Hallucination Mitigation Leveraging our unified reasoning, SkiLa can implicitly zoom in on key image regions to acquire fine-grained information, shown in Figure 6. This process effectively mitigates hallucinations on visual details, such as correctly identifying all four white pillows, while circumventing the latency associated with complex and explicit tool invocations.

Adaptive Unified Reasoning Figure 7 demonstrates that SkiLa exhibits adaptive unified reasoning capability. The task requires the model to accurately detect and localize the target, and then select the optimal bounding box from two candidates. The upper example shows SkiLa effortlessly identifies the target through a single-step unified reasoning process. In contrast, for a more challenging case, the lower case, where the two candidate boxes exhibit significant overlap and both receive high confidence scores, SkiLa adaptively performs two sequential reasoning steps to discern subtle distinctions and ultimately select the correct box. This illustrates SkiLa’s ability to dynamically adjust its reasoning depth based on task difficulty.

5. Conclusion

In this work, we introduced Sketch-in-Latents (SkiLa), a novel unified reasoning paradigm that enables MLLMs to think in a unified manner through a hybrid autoregressive process. It dynamically alternates between the textual thinking mode to generate textual thoughts and the visual sketching mode to generate latent sketch tokens as visual thoughts. A latent visual semantics reconstruction mechanism is proposed to ensure that the latent sketch tokens are semantically grounded. Extensive experiments demonstrate that SkiLa achieves superior performance on vision-centric tasks while exhibiting strong generalization to diverse general multi-modal benchmarks. Our future work will develop models that autonomously select the optimal reasoning pattern among textual, visual, and joint, in a task-adaptive manner.

References

- [1] Josh Achiam, Steven Adler, Sandhini Agarwal, Lama Ahmad, Ilge Akkaya, Florencia Leoni Aleman, Diogo Almeida, Janko Altenschmidt, Sam Altman, Shyamal Anadkat, et al. Gpt-4 technical report. *arXiv preprint arXiv:2303.08774*, 2023. 5
- [2] Jinze Bai, Shuai Bai, Yunfei Chu, Zeyu Cui, Kai Dang, Xiaodong Deng, Yang Fan, Wenbin Ge, Yu Han, Fei Huang, et al. Qwen technical report. *arXiv preprint arXiv:2309.16609*, 2023. 1
- [3] Shuai Bai, Keqin Chen, Xuejing Liu, Jialin Wang, Wenbin Ge, Sibong Song, Kai Dang, Peng Wang, Shijie Wang, Jun Tang, et al. Qwen2. 5-vl technical report. *arXiv preprint arXiv:2502.13923*, 2025. 1, 5
- [4] Lin Chen, Jinsong Li, Xiaoyi Dong, Pan Zhang, Yuhang Zang, Zehui Chen, Haodong Duan, Jiaqi Wang, Yu Qiao, Dahua Lin, et al. Are we on the right way for evaluating large vision-language models? *Advances in Neural Information Processing Systems*, 37:27056–27087, 2024. 5
- [5] Xiaokang Chen, Zhiyu Wu, Xingchao Liu, Zizheng Pan, Wen Liu, Zhenda Xie, Xingkai Yu, and Chong Ruan. Januspro: Unified multimodal understanding and generation with data and model scaling. *arXiv preprint arXiv:2501.17811*, 2025. 2, 3, 5
- [6] Jeffrey Cheng and Benjamin Van Durme. Compressed chain of thought: Efficient reasoning through dense representations. *arXiv preprint arXiv:2412.13171*, 2024. 3
- [7] Wei-Lin Chiang, Zhuohan Li, Zi Lin, Ying Sheng, Zhanghao Wu, Hao Zhang, Lianmin Zheng, Siyuan Zhuang, Yonghao Zhuang, Joseph E Gonzalez, et al. Vicuna: An open-source chatbot impressing gpt-4 with 90%* chatgpt quality, march 2023. URL <https://lmsys.org/blog/2023-03-30-vicuna>, 3(5), 2023. 1
- [8] Chaorui Deng, Deyao Zhu, Kunchang Li, Chenhui Gou, Feng Li, Zeyu Wang, Shu Zhong, Weihao Yu, Xiaonan Nie, Ziang Song, et al. Emerging properties in unified multimodal pretraining. *arXiv preprint arXiv:2505.14683*, 2025. 2, 3
- [9] Haodong Duan, Junming Yang, Yuxuan Qiao, Xinyu Fang, Lin Chen, Yuan Liu, Xiaoyi Dong, Yuhang Zang, Pan Zhang, Jiaqi Wang, et al. Vlmevalkit: An open-source toolkit for evaluating large multi-modality models. In *Proceedings of the 32nd ACM International Conference on Multimedia*, pages 11198–11201, 2024. 5
- [10] Martha J Farah. Psychophysical evidence for a shared representational medium for mental images and percepts. *Journal of Experimental Psychology: General*, 114(1):91, 1985. 2
- [11] Chaoyou Fu, Peixian Chen, Yunhang Shen, Yulei Qin, Mengdan Zhang, Xu Lin, Jinrui Yang, Xiawu Zheng, Ke Li, Xing Sun, et al. Mme: A comprehensive evaluation benchmark for multimodal large language models. In *The Thirtieth Annual Conference on Neural Information Processing Systems Datasets and Benchmarks Track*, 2025. 6
- [12] Xingyu Fu, Yushi Hu, Bangzheng Li, Yu Feng, Haoyu Wang, Xudong Lin, Dan Roth, Noah A Smith, Wei-Chiu Ma, and Ranjay Krishna. Blink: Multimodal large language models can see but not perceive. In *European Conference on Computer Vision*, pages 148–166. Springer, 2024. 2, 5
- [13] Shibo Hao, Sainbayar Sukhbaatar, DiJia Su, Xian Li, Zhiting Hu, Jason Weston, and Yuandong Tian. Training large language models to reason in a continuous latent space. *arXiv preprint arXiv:2412.06769*, 2024. 2, 3
- [14] Jack Hong, Shilin Yan, Jiayin Cai, Xiaolong Jiang, Yao Hu, and Weidi Xie. Worldsense: Evaluating real-world omnimodal understanding for multimodal llms. *arXiv preprint arXiv:2502.04326*, 2025. 2
- [15] Yushi Hu, Weijia Shi, Xingyu Fu, Dan Roth, Mari Ostendorf, Luke Zettlemoyer, Noah A Smith, and Ranjay Krishna. Visual sketchpad: Sketching as a visual chain of thought for multimodal language models. *Advances in Neural Information Processing Systems*, 37:139348–139379, 2024. 2, 3
- [16] Wenxuan Huang, Bohan Jia, Zijie Zhai, Shaosheng Cao, Zheyu Ye, Fei Zhao, Zhe Xu, Yao Hu, and Shaohui Lin. Vision-r1: Incentivizing reasoning capability in multimodal large language models. *arXiv preprint arXiv:2503.06749*, 2025. 1, 2, 5, 6
- [17] Stephen M Kosslyn. *Image and brain: The resolution of the imagery debate*. MIT press, 1996. 2
- [18] Ang Li, Charles Wang, Deqing Fu, Kaiyu Yue, Zikui Cai, Wang Bill Zhu, Ollie Liu, Peng Guo, Willie Neiswanger, Furong Huang, et al. Zebra-cot: A dataset for interleaved vision language reasoning. *arXiv preprint arXiv:2507.16746*, 2025. 5
- [19] Bangzheng Li, Ximeng Sun, Jiang Liu, Ze Wang, Jialian Wu, Xiaodong Yu, Hao Chen, Emad Barsoum, Muhao Chen, and Zicheng Liu. Latent visual reasoning. *arXiv preprint arXiv:2509.24251*, 2025. 3, 5, 6
- [20] Chengzu Li, Wenshan Wu, Huanyu Zhang, Yan Xia, Shaoguang Mao, Li Dong, Ivan Vulić, and Furu Wei. Imagine while reasoning in space: Multimodal visualization-of-thought. *arXiv preprint arXiv:2501.07542*, 2025. 2, 3
- [21] Junnan Li, Dongxu Li, Silvio Savarese, and Steven Hoi. Bliip-2: Bootstrapping language-image pre-training with frozen image encoders and large language models. In *International conference on machine learning*, pages 19730–19742. PMLR, 2023. 1
- [22] Pengxiang Li, Shilin Yan, Joey Tsai, Renrui Zhang, Ruichuan An, Ziyu Guo, and Xiaowei Gao. Adaptive

- classifier-free guidance via dynamic low-confidence masking. *arXiv preprint arXiv:2505.20199*, 2025. 2
- [23] Yifan Li, Yifan Du, Kun Zhou, Jinpeng Wang, Wayne Xin Zhao, and Ji-Rong Wen. Evaluating object hallucination in large vision-language models. *arXiv preprint arXiv:2305.10355*, 2023. 6
- [24] Haotian Liu, Chunyuan Li, Qingyang Wu, and Yong Jae Lee. Visual instruction tuning. *Advances in neural information processing systems*, 36:34892–34916, 2023. 1
- [25] Haotian Liu, Chunyuan Li, Yuheng Li, Bo Li, Yuanhan Zhang, Sheng Shen, and Yong Jae Lee. Llava-next: Improved reasoning, ocr, and world knowledge, 2024. 5
- [26] Yuan Liu, Haodong Duan, Yuanhan Zhang, Bo Li, Songyang Zhang, Wangbo Zhao, Yike Yuan, Jiaqi Wang, Conghui He, Ziwei Liu, et al. Mmbench: Is your multi-modal model an all-around player? In *European conference on computer vision*, pages 216–233. Springer, 2024. 5
- [27] Yuqi Liu, Tianyuan Qu, Zhisheng Zhong, Bohao Peng, Shu Liu, Bei Yu, and Jiaya Jia. Visionreasoner: Unified visual perception and reasoning via reinforcement learning. *arXiv preprint arXiv:2505.12081*, 2025. 2
- [28] Ziyu Liu, Zeyi Sun, Yuhang Zang, Xiaoyi Dong, Yuhang Cao, Haodong Duan, Dahua Lin, and Jiaqi Wang. Visual-rl: Visual reinforcement fine-tuning. *arXiv preprint arXiv:2503.01785*, 2025. 1, 2
- [29] Hao Shao, Shengju Qian, Han Xiao, Guanglu Song, Zhuofan Zong, Letian Wang, Yu Liu, and Hongsheng Li. Visual cot: Unleashing chain-of-thought reasoning in multi-modal language models. *CoRR*, 2024. 2, 3
- [30] Zhenyi Shen, Hanqi Yan, Linhai Zhang, Zhanghao Hu, Yali Du, and Yulan He. Codi: Compressing chain-of-thought into continuous space via self-distillation. *arXiv preprint arXiv:2502.21074*, 2025. 3
- [31] Amanpreet Singh, Vivek Natarajan, Meet Shah, Yu Jiang, Xinlei Chen, Dhruv Batra, Devi Parikh, and Marcus Rohrbach. Towards vqa models that can read. In *Proceedings of the IEEE/CVF conference on computer vision and pattern recognition*, pages 8317–8326, 2019. 6
- [32] Chameleon Team. Chameleon: Mixed-modal early-fusion foundation models. *arXiv preprint arXiv:2405.09818*, 2024. 2
- [33] Gemma Team, Aishwarya Kamath, Johan Ferret, Shreya Pathak, Nino Vieillard, Ramona Merhej, Sarah Perrin, Tatiana Matejovicova, Alexandre Ramé, Morgane Rivière, et al. Gemma 3 technical report. *arXiv preprint arXiv:2503.19786*, 2025. 5
- [34] Shengbang Tong, Zhuang Liu, Yuexiang Zhai, Yi Ma, Yann LeCun, and Saining Xie. Eyes wide shut? exploring the visual shortcomings of multimodal llms. In *Proceedings of the IEEE/CVF Conference on Computer Vision and Pattern Recognition*, pages 9568–9578, 2024. 5
- [35] Hugo Touvron, Thibaut Lavril, Gautier Izacard, Xavier Martinet, Marie-Anne Lachaux, Timothée Lacroix, Baptiste Rozière, Naman Goyal, Eric Hambro, Faisal Azhar, et al. Llama: Open and efficient foundation language models. *arXiv preprint arXiv:2302.13971*, 2023. 1
- [36] Michael Tschannen, Alexey Gritsenko, Xiao Wang, Muhammad Ferjad Naeem, Ibrahim Alabdulmohsin, Nikhil Parthasarathy, Talfan Evans, Lucas Beyer, Ye Xia, Basil Mustafa, et al. Siglip 2: Multilingual vision-language encoders with improved semantic understanding, localization, and dense features. *arXiv preprint arXiv:2502.14786*, 2025. 5
- [37] Haochen Wang, Anlin Zheng, Yucheng Zhao, Tiancai Wang, Zheng Ge, Xiangyu Zhang, and Zhaoxiang Zhang. Reconstructive visual instruction tuning. *arXiv preprint arXiv:2410.09575*, 2024. 5, 6
- [38] Haozhe Wang, Chao Qu, Zuming Huang, Wei Chu, Fangzhen Lin, and Wenhui Chen. VI-rethinker: Incentivizing self-reflection of vision-language models with reinforcement learning. *arXiv preprint arXiv:2504.08837*, 2025. 1, 2
- [39] Wenbin Wang, Liang Ding, Minyan Zeng, Xiabin Zhou, Li Shen, Yong Luo, Wei Yu, and Dacheng Tao. Divide, conquer and combine: A training-free framework for high-resolution image perception in multimodal large language models. In *Proceedings of the AAAI Conference on Artificial Intelligence*, pages 7907–7915, 2025. 5
- [40] Weiyun Wang, Zhangwei Gao, Lixin Gu, Hengjun Pu, Long Cui, Xingguang Wei, Zhaoyang Liu, Linglin Jing, Shenglong Ye, Jie Shao, et al. Internvl3. 5: Advancing open-source multimodal models in versatility, reasoning, and efficiency. *arXiv preprint arXiv:2508.18265*, 2025. 1
- [41] Jason Wei, Xuezhi Wang, Dale Schuurmans, Maarten Bosma, Fei Xia, Ed Chi, Quoc V Le, Denny Zhou, et al. Chain-of-thought prompting elicits reasoning in large language models. *Advances in neural information processing systems*, 35:24824–24837, 2022. 1, 2
- [42] Penghao Wu and Saining Xie. V*: Guided visual search as a core mechanism in multimodal llms, 2023. [URL https://arxiv.org/abs/2312.14135](https://arxiv.org/abs/2312.14135), 5. 2, 3
- [43] Penghao Wu and Saining Xie. V?: Guided visual search as a core mechanism in multimodal llms. In *Proceedings of the IEEE/CVF Conference on Computer Vision and Pattern Recognition*, pages 13084–13094, 2024. 5
- [44] XAI. Grok-1.5 vision preview, 2024. 5
- [45] Yi Xu, Chengzu Li, Han Zhou, Xingchen Wan, Caiqi Zhang, Anna Korhonen, and Ivan Vulić. Visual planning: Let’s think only with images. *arXiv preprint arXiv:2505.11409*, 2025. 2, 3
- [46] Shilin Yan, Jiaming Han, Joey Tsai, Hongwei Xue, Rongyao Fang, Lingyi Hong, Ziyu Guo, and Ray Zhang. Crosslmm: Decoupling long video sequences from llms via dual cross-attention mechanisms. *arXiv preprint arXiv:2505.17020*, 2025. 2
- [47] Zeyuan Yang, Xueyang Yu, Delin Chen, Maohao Shen, and Chuang Gan. Machine mental imagery: Empower multimodal reasoning with latent visual tokens. *arXiv preprint arXiv:2506.17218*, 2025. 3
- [48] En Yu, Kangheng Lin, Liang Zhao, Jisheng Yin, Yana Wei, Yuang Peng, Haoran Wei, Jianjian Sun, Chunrui Han, Zheng Ge, et al. Perception-rl: Pioneering perception policy with reinforcement learning. *arXiv preprint arXiv:2504.07954*, 2025. 1, 2
- [49] Yi-Fan Zhang, Huanyu Zhang, Haochen Tian, Chaoyou Fu, Shuangqing Zhang, Junfei Wu, Feng Li, Kun Wang, Qingsong Wen, Zhang Zhang, et al. Mme-realworld: Could

- your multimodal llm challenge high-resolution real-world scenarios that are difficult for humans? *arXiv preprint arXiv:2408.13257*, 2024. 5
- [50] Yi-Fan Zhang, Xingyu Lu, Shukang Yin, Chaoyou Fu, Wei Chen, Xiao Hu, Bin Wen, Kaiyu Jiang, Changyi Liu, Tianke Zhang, et al. Thyme: Think beyond images. *arXiv preprint arXiv:2508.11630*, 2025. 2
- [51] Zhuosheng Zhang, Aston Zhang, Mu Li, Hai Zhao, George Karypis, and Alex Smola. Multimodal chain-of-thought reasoning in language models. *arXiv preprint arXiv:2302.00923*, 2023. 1
- [52] Zhen Zhang, Xuehai He, Weixiang Yan, Ao Shen, Chenyang Zhao, Shuohang Wang, Yelong Shen, and Xin Eric Wang. Soft thinking: Unlocking the reasoning potential of llms in continuous concept space. *arXiv preprint arXiv:2505.15778*, 2025. 3
- [53] Shitian Zhao, Haoquan Zhang, Shaoheng Lin, Ming Li, Qilong Wu, Kaipeng Zhang, and Chen Wei. Pyvision: Agentic vision with dynamic tooling. *arXiv preprint arXiv:2507.07998*, 2025. 2, 3
- [54] Ziwei Zheng, Michael Yang, Jack Hong, Chenxiao Zhao, Guohai Xu, Le Yang, Chao Shen, and Xing Yu. Deep-eyes: Incentivizing” thinking with images” via reinforcement learning. *arXiv preprint arXiv:2505.14362*, 2025. 2, 3

Sketch-in-Latents: Eliciting Unified Reasoning in MLLMs

Supplementary Material

6. Training Data Details

Our SFT training data is curated from the Zebra-CoT, which is a diverse large-scale dataset with 182K samples, containing logically coherent interleaved text-image reasoning traces. We filter this dataset to select samples suitable for SkiLa training, excluding 3D data and instances where the intermediate sketch images are too complex for the MLLM to effectively learn to reconstruct. Consequently, our training dataset contains 101K samples. Our detailed statistics of training dataset is shown in Table 4.

Category	Count	Percentage (%)
Visual Jigsaw	21,899	21.6
Visual Search	30,000	29.6
Geometry	1,058	1.1
Checkers	2,753	2.7
Chess	20,483	20.2
Connect Four	2,029	2.0
Maze	20,000	19.8
RPM	3,000	3.0
Total	101,222	100.0

Table 4. Detailed statistics of training data.

7. Choice of Loss Function

We evaluate different loss functions for latent sketch reconstruction. Cosine similarity focuses solely on directional alignment between feature vectors, whereas mean squared error (MSE) explicitly minimizes the reconstruction error between generated and target latent sketches. As shown in Table 5, MSE consistently yields higher performance. This is because latent visual representations encode semantics through both direction and magnitude: direction captures coarse alignment in the feature space, while magnitude carries fine-grained visual cues. Cosine similarity, which ignores magnitude differences, may therefore miss subtle but important details. In contrast, MSE preserves both components of the latent features, enabling more precise and faithful visual reconstructions.

8. More Cases

In the main text, we showed a subset of examples demonstrating SkiLa’s effectiveness. Here, we include additional and broader cases across more task types.

Choice of Loss	MME-RealWorld-Lite		
	Perception	Reasoning	Overall
cosine similarity loss	56.1	48.5	53.1
mean squared error loss	56.6	50.2	54.1

Table 5. Impact of different loss functions for the latent sketch reconstruction loss.

Fine-Grained Visual Grounding. As shown in Figure 8, SkiLa’s unified latent reasoning enables it to internally focus on key regions of an image and recover fine-grained visual details without relying on external tools. This internal refinement allows SkiLa to correctly identify subtle attributes, such as recognizing that all three glasses contain water, while avoiding the latency introduced by explicit region-based operations. Conventional models often overlook such details or produce hallucinated predictions due to insufficient visual grounding.

Latent Scene Completion. As illustrated in Figure 9, SkiLa can reconstruct the missing content of a partially occluded image within its latent sketch space and determine which candidate completion is semantically consistent with the underlying scene. This ability to integrate fragmented visual information enables SkiLa to recover the correct jigsaw piece. In contrast, Vision-R1 incorrectly identifies the missing part because it struggles to form a coherent global scene from the incomplete visual input.

Cross-Image Visual Alignment. As shown in Figure 10, SkiLa conducts unified reasoning directly over fine-grained visual semantics. In this example, SkiLa-U accurately aligns the “REF” marker with the cat’s front paw by reconstructing its precise spatial location across images. In contrast, Vision-R1 matches only at a coarse body-level region and therefore predicts incorrectly. This demonstrates that SkiLa not only captures subtle cross-image correspondences but also integrates them seamlessly into its subsequent textual reasoning.

Multi-Round Visual Refinement. SkiLa demonstrates the ability to perform detailed, multi-step visual reasoning by iteratively examining and comparing regions of interest. As shown in Figure 11, it inspects the two points across multiple rounds, progressively focusing on their local visual properties. By integrating observations step by step, SkiLa accurately determines that the points have similar colors. In contrast, Vision-R1 relies on a coarse global judgment and predicts incorrectly. This case illustrates how SkiLa can conduct stepwise, focused analysis to capture subtle visual features that conventional models often miss.

	<p>Vision-R1: <code><think></code> The image displays there are three glasses on the table. Two of them have clear liquid, which is water. The third one is empty. The question is asking how many glasses are filled with water. So, the answer should be two. The options are A to D, with D being 2. <code></think></code> <code><answer></code> Final Answer: D <code></answer></code> ✘</p>
<p>Question: How many glasses are filled with water? (A) 5 (B) 3 (C) 4 (D) 2? Answer: (B)</p>	<p>SkiLa: <code><think></code>The problem asks to count the number of glasses containing water in the provided image. I need to carefully examine each glass present on the table. To accurately identify and count the glasses with water, I will focus on the area around the pizza and the table setting. <code></think></code> <code>< sketch_start >< skila >*27< sketch_end ></code> <code><think></code>The zoomed-in view clearly shows three glasses on the table: one next to the pizza, one near the top right, and another at the bottom left. All three glasses appear to contain clear liquid, which is consistent with water. Based on this detailed observation, there are three glasses filled with water. <code></think></code> <code><answer></code>B <code></answer></code> ✓</p>

Figure 8. A case study demonstrates fine-grained visual grounding capability of SkiLa.

	<p>Vision-R1: <code><think></code> The user is asking which image is the missing part in the first image. The options are A (the second image) or B (the third image). From the image provided, the first image is incomplete and lacks the vertical structure with cranes that's shown in the third image. The second image shows the ship from a different angle but doesn't include the cranes. The third image specifically displays the vertical structure with cranes, which is missing from the first image. So the missing part in the first image must be the third image. Therefore, the answer should be B. <code></think></code> <code><answer></code> B <code></answer></code> ✘</p>
 <p>Question: Which image is the missing part in the first image? (A) the second image (B) the third image Answer: (A)</p>	<p>SkiLa-U: <code><think></code>The problem asks to identify which image completes the scene shown in the first image. I need to compare the missing section of the first image with the provided options. To determine the missing part, I will visualize the complete scene without the black box covering it. <code></think></code> <code>< sketch_start >< skila >*27< sketch_end ></code> <code><think></code>The reconstructed image shows the full scene. Comparing this with the original image and the options, the missing area corresponds to the second image. The second image contains the parts that were obscured by the black box in the first image. <code></think></code> <code><answer></code>A <code></answer></code> ✓</p>

Figure 9. A case study demonstrates latent scene completion capability of SkiLa.

	<p>Question: Which point is corresponding to the reference point? (A) Point A (B) Point B (C) Point C (D) Point D Answer: (D)</p>
	<p>Vision-R1: <code><think></code> The question is asking which point corresponds to the reference point. The image displays that in the first image, there's a reference point labeled "REF" near the cat's body. Then, in the second image, there are points A, B, C, D marked on the cat. The key detail here is that Point C is located in the same area as the reference point "REF" in the first image. So, the reference point from the first image is at Point C in the second image. The answer should be C. <code></think></code> <code><answer></code> Final Answer: C <code></answer></code> ✘</p> <p>SkiLa: <code><think></code>The problem asks to identify which point in the second image corresponds to the "REF" marker visible in the first image. To accurately match the reference point, I need to locate its position relative to the cat and the furniture in the second image. <code></think></code> <code>< sketch_start >< skila >*27< sketch_end ></code> <code><think></code>The visual thought clearly shows the red circle labeled "REF" on the table surface in the first image. In the second image, this corresponds to the area where the cat's paws are resting on the black surface. Comparing the location of the "REF" marker in the first image to the points marked on the cat in the second image, it aligns with the cat's front right paw (point D). <code></think></code> <code><answer></code>D <code></answer></code> ✓</p>

Figure 10. A case study demonstrates cross-image visual correspondence alignment capability of SkiLa.

	<p>Question: Consider the surface color (color without shading) of the two points in the image. Which one is darker, or the color is about the same? (A) A is darker (B) B is darker (C) About the same Answer: (C)</p> <hr/> <p>Vision-R1: <code><think></code> The image displays that point A is on a blue pot and point B is on a red pot. The blue pot is on the lower shelf, and the red pot is on the upper shelf. The key detail here is that the blue pot (point A) appears darker in color compared to the red pot (point B) <code></think></code> <code><answer></code> Final Answer: A <code></answer></code> ✘</p> <hr/> <p>SkiLa: <code><think></code> The problem asks to compare the colors of two points, A and B, shown in the image. To accurately determine which point has a darker color, I need to visually inspect the area around each letter. I will focus on the region containing the letter 'A'.<code></think></code> <code>< sketch_start >< skila >*27< sketch_end ></code> <code><think></code> Observing the zoomed-in view of point A, it appears to be a light gray or off-white color. Now, I will examine the region around point B.<code></think></code> <code>< sketch_start >< skila >*27< sketch_end ></code> <code><think></code> The zoomed-in view of point B also shows a similar light gray or off-white color. Both points A and B exhibit very similar shades of color. Based on this visual comparison, the colors at both points appear to be about the same.<code></think></code> <code><answer></code>C<code></answer></code> ✓</p>
------------------------------------------------------------------------------------	-----------------------------------------------------------------------------------------------------------------------------------------------------------------------------------------------------------------------------------------------------------------------------------------------------------------------------------------------------------------------------------------------------------------------------------------------------------------------------------------------------------------------------------------------------------------------------------------------------------------------------------------------------------------------------------------------------------------------------------------------------------------------------------------------------------------------------------------------------------------------------------------------------------------------------------------------------------------------------------------------------------------------------------------------------------------------------------------------------------------------------------------------------------------------------------------------------------------------------------------------------------------------------------------------------------------------------------------------------------------------------------------------------------------------------------------------------------------------------------------------------------------------------------------------------------------------------------------------------------------------------------------------------------------------------------------------------------------------------------------------------------------------------------

Figure 11. A case study demonstrates multi-round visual refinement capability of SkiLa.